Supplement information for "Lattice Distortion-Enhanced Superlubricity of (Mo, X)S_2 (X= Al, Ti, V and Cr) with Moiré Superlattice"

Peixuan Li [a, #], Jiaqi Lu [a, b, #], William Yi Wang[a,c,*], Xudong Sui [d,*], Chengxiong Zou [a, c], Ying Zhang [a], Jun Wang [a, c, *], Deye Lin[e], Zhibin Lu [d], Haifeng Song [f], Xiaoli Fan [a], Junying Hao [d], Jinshan Li [a, c], Weimin Liu [a]

[a.] State Key Laboratory of Solidification Processing, Northwestern Polytechnical University, Xi'an, 710072, China.
[b.] School of Science, Shenyang Ligong University, Liaoning, 110159, China.
[c.] Chongqing Innovation Center of Northwestern Polytechnical University, 401135, Chongqing
[d.] State Key Laboratory of Solid Lubrication, Lanzhou Institute of Chemical Physics, Chinese Academy of Science, 730000, Lanzhou.
[e.] CAEP Software Center for High Performance Numerical Simulation, Beijing, 100088, China
[f.] Laboratory of Computational Physics, Institute of Applied Physics and Computational Mathematics, Beijing, 100088, China
[#] Equal to contribution.
Email: wywang@nwpu.edu.cn ; nwpuwj@nwpu.edu.cn; suixudong@licp.cas.cn

The 2D contour plots of bonding charge density of pure MoS_2 with the twisted angles of 13.17°, 21.79° and 32.20°, respectively are shown in **Fig. S1.**, which indicates the movement of interlayer S atoms. Interlayer S-S repulsion in the AA stacking, where the top layer S atom sits almost above a bottom layer S atom, is improved, and in AB stacking (Bernal stacking) area are weakened. This change of intralayer Mo-S bonds generates the layer corrugations in **Fig. S2.**. Thus, the larger twisted angles in the period range of 0°~30°, the smaller areas of AA stacking are formed which results in the low corrugations of layers, corresponding to the previous studies[1-2].

Fig. S3-**Fig. S5** display the 2D contour plots and 3D isosuface of bonding charge density of non-twisted (Mo, X)S_2 (X= Al, Ti, V and Cr). It is acknowledged that van der Waals (vdW) interactions is influenced by the polarizable bond. One the one hand, the p-type doping for Al, Ti and V result in less polarizable S atoms in the interface layer and lower vdW interactions between interlayer[3-5]. On the other hand, the electronegativity difference of X-S (X= Al, Ti, V and Cr) is larger than Mo-S, which implys the stronger polarization of X-S. Since interlayer balance between the S-S hybridization and vdW interactions are broken by the above two competitive factors, atoms are impelled in the direction of perpendicular 2D-plane and the layer deformations are formed. Due to the less polarizable S atoms at the interface for (Mo, X)S_2 (X= Al, Ti), the vdW force decreases and the doped positions peaks at Mo atom layer. Especially, a few bonding charge around the p-orbital element of Al in **Fig. S3**, indicates extreme weak bonding strength, resulting drastic fluctuation of Mo layer. **Fig. S4** shows that the Cr atom is pushed at the bottom point of Mo atom layer owing to the larger vdW attractions by stronger polarizable bonds of Cr-S (1.66-2.58 for Cr-S and 2.16-2.58 for Mo-S, respectively). The V atom also locates at the bottom of Mo layer, which could be attributed to the effect of electronegativity difference is higher than p-type doping.

The schematic diagram of the deposition process for (Mo, X)S_2 (X=Al, Ti, V, Cr) with non-twisted as shown in **Fig. S6**. In addition, the originally experimental data and computational structures have been attached in separate files.

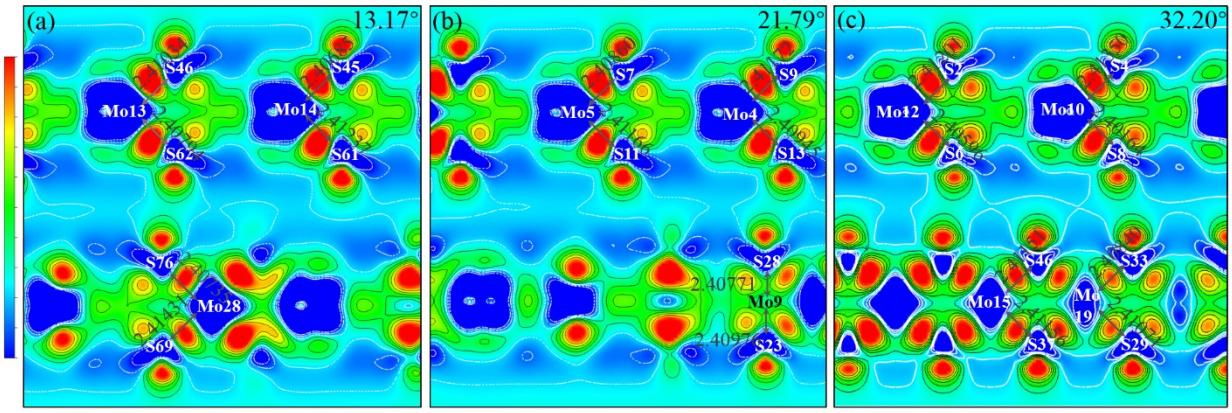

Fig. S1 The 2D contour plots of bonding charge density (Δρ) of the twisted angle of 13.17°, 21.79° and 32.20° MoS_2. The bonding length of Mo-S, Mo and S atoms in feature sites are labelled and Δρ = -0.0005~0.013$e^{-1}Å^{-3}$.

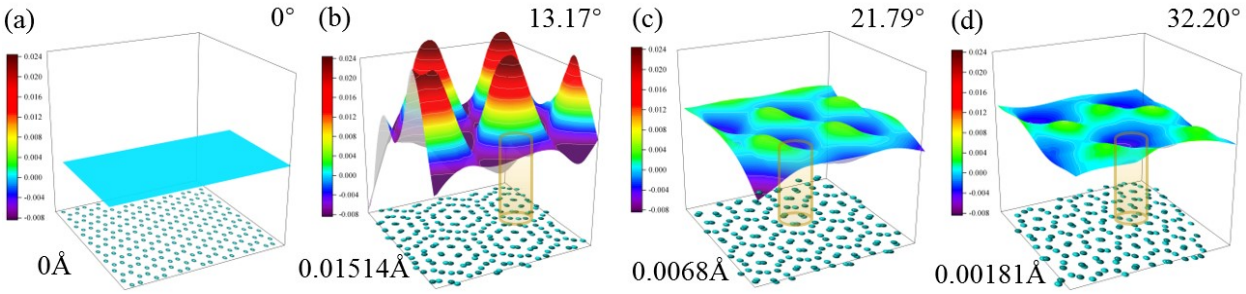

Fig. S2 The corrugation of Mo-atom in the up layer along the direction of z axis. (a) is the as-built pure-0° MoS_2, and (b-d) show the twisted angle of 13.17°, 21.79°and 32.20°MoS_2,respectively.

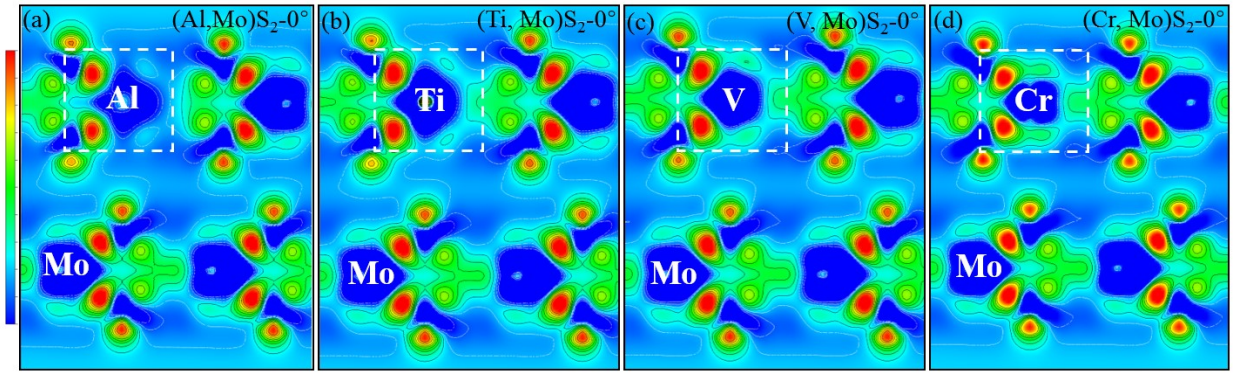

Fig. S3 The 2D contour plots of bonding charge density (Δρ) of (a) (Al, Mo)S_2-0°, (b) (Ti, Mo)S_2-0°, (c) (V, Mo)S_2-0°and (d) (Cr, Mo)S_2-0° structures.The X (X=Al, Ti, V, Cr) and Mo atoms in feature sites are labelled and of Δρ = -0.005~0.018$e^{-1}Å^{-3}$.

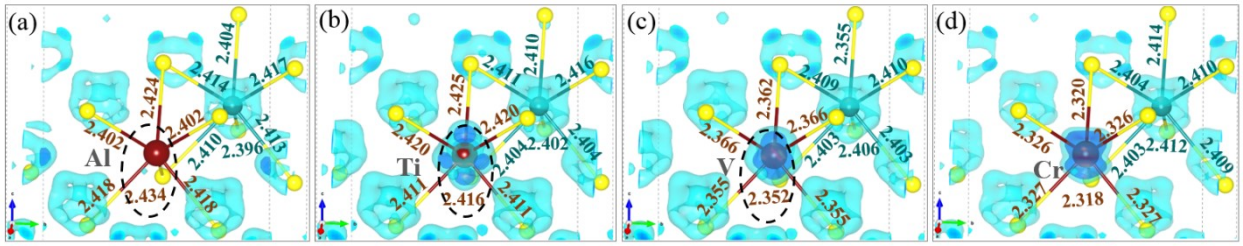

Fig. S4 3D isosurfaces of Δρ are applied to characterize the non-twisted (Mo, X)S_2 (X= Al, Ti, V and Cr). The Δρ= -0.02,-0.03 e-$^{1}Å^{-3}$ isosurface are ploted in cyan and blue colors respectively, which identify the atomic sites contributing electrons (Δρ < 0). The bonding length of Mo-S and X-S (X=Al, Ti, V, Cr) are labelled.

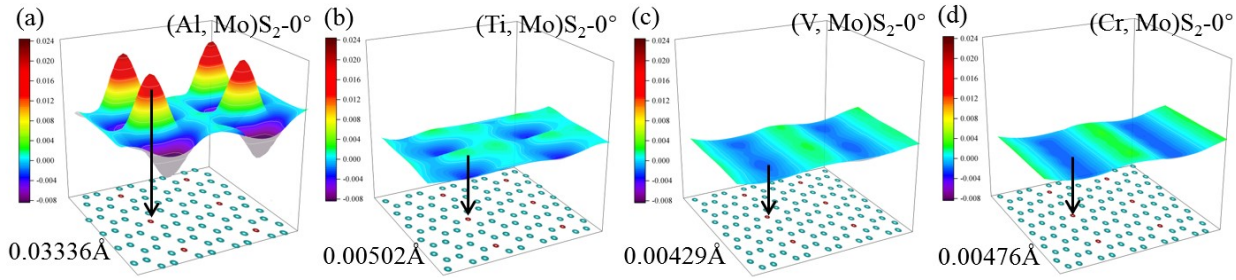

Fig. S5 The corrugation of Mo-atom in the up layer of non-twisted (Mo, X)S_2 (X= Al, Ti, V and Cr) along the z axis direction.

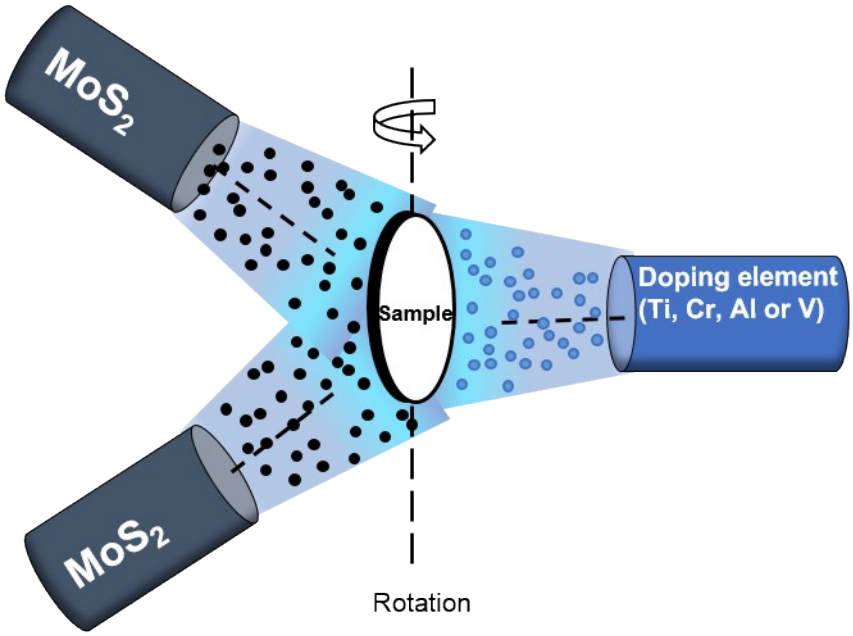

Fig. S6 Schematic diagram of the deposition process for (Mo, X)S_2 (X= Al, Ti, V, Cr) with non-twisted in this work.

Reference

1 M. M. van Wijk; Schuring, A.; Katsnelson, M. I., et al., Relaxation of moiré patterns for slightly misaligned identical lattices: graphene on graphite. 2D Mater., 2015, 2, 034010.

2 Uchida, K.; Furuya, S.; Iwata, J.-I., et al., Atomic corrugation and electron localization due to moiré patterns in twisted bilayer graphenes. Phys. Rev. B, 2014, 90, 155451.

3 Kong, L.; Zhao, Y.; Dasgupta, B., et al., Minimizing isolate catalyst motion in metal-assisted chemical etching for deep trenching of silicon nanohole array. ACS Appl. Mater. Interfaces, 2017, 9, 20981-20990.

4 Tsoi, S.; Dev, P.; Friedman, A. L., et al., Van der Waals screening by single-layer graphene and molybdenum disulfide. ACS Nano, 2014, 8, 12410-12417.

5 Huttmann, F.; Martinez-Galera, A. J.; Caciuc, V., et al., Tuning the van der Waals interaction of graphene with molecules via doping. Phys. Rev. Lett., 2015, 115, 236101.